AD-A082 623 RENSSELAER POLYTECHNIC INST TROY NY DEPT OF MECHANIC--ETC F/G 11/6
THE RATE (TIME)-DEPENDENT BEHAVIOR OF TI-7AL-8CB-1TA TITANIUM A--ETC(U)
DEC 79 D KUJAWSKI, E KREMPL N00014-76-C-0231
UNCLASSIFIED RPI-CE-79-8 NL

END
DATE FILMED
5-80
DTIC

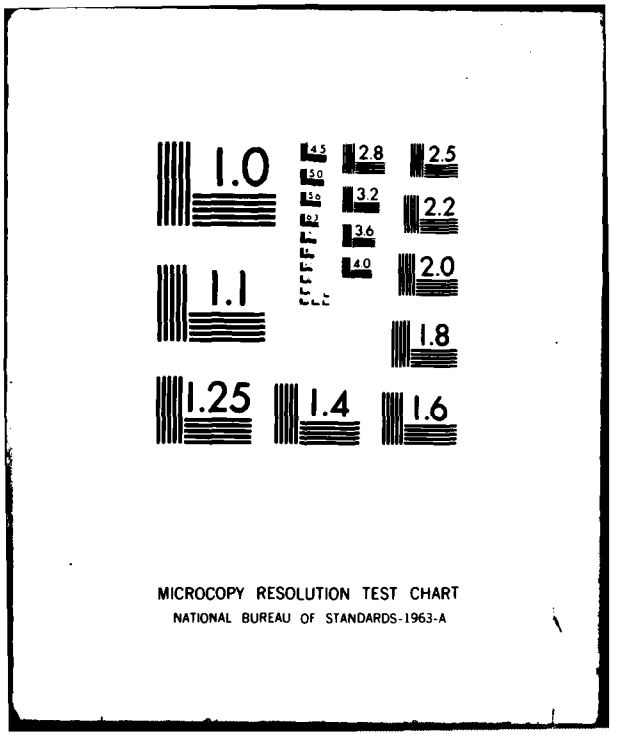
1.0
1.1
1.25
1.4
1.6
1.8
2.0
2.2
2.5
2.8
3.2
3.6
4.0
4.5
5.0
5.6
6.3
7.1
MICROCOPY RESOLUTION TEST CHART
NATIONAL BUREAU OF STANDARDS-1963-A

THE RATE (TIME)-DEPENDENT BEHAVIOR OF Ti-7Al-2Cb-1Ta TITANIUM ALLOY AT ROOM TEMPERATURE UNDER QUASISTATIC MONOTONIC AND CYCLIC LOADING

(10)
D. Kujawski and E. Krempl
Department of Mechanical Engineering,
Aeronautical Engineering & Mechanics
Rensselaer Polytechnic Institute
Troy, New York 12181

(2)

(6) THE RATE (TIME)-DEPENDENT BEHAVIOR OF Ti-7Al-2Cb-1Ta TITANIUM ALLOY AT ROOM TEMPERATURE UNDER QUASISTATIC MONOTONIC AND CYCLIC LOADING

(10) D. Kujawski* and E. Krempl
Department of Mechanical Engineering,
Aeronautical Engineering & Mechanics
Rensselaer Polytechnic Institute
Troy, New York 12181

(14) Report No. RPI-CS-79-5
(11) December 1979
(12) 41
(15) N00014-76-C-0231

*On leave from the Technical University of Warsaw, Poland.

THE RATE (TIME)-DEPENDENT BEHAVIOR OF Ti-7Al-2Cb-1Ta TITANIUM ALLOY AT ROOM TEMPERATURE UNDER QUASISTATIC MONOTONIC AND CYCLIC LOADING

D. Kujawski and E. Krempl
Department of Mechanical Engineering,
Aeronautical Engineering & Mechanics
Rensselaer Polytechnic Institute
Troy, New York 12181

ABSTRACT

Uniaxial tests using a servocontrolled testing machine and strain measurement at the gage length were performed on a high-strength, low-ductility, Titanium Alloy. Tests involved monotonic and cyclic loadings with strain rates between 2×10^{-8} to 10^{-3} s^{-1}, stress rates from 10^{-2} to 10^{2} MPa s^{-1} and short-term relaxation and creep tests. The inelastic behavior is strongly rate-dependent. Ratchetting is shown to increase as the stress rate decreases. No strain-rate history effect was found. A unique stress-strain curve is ultimately reached for a given strain rate irrespective of prior history as long as only positive stresses are imposed. In the plastic range the relaxation drop in a given time period depends only on the strain rate preceding the test and is independent of the actual stress and strain. The results are qualitatively in accordance with the viscoplasticity theory based on total strain and overstress.

INTRODUCTION

Stress-strain curves obtained under dynamic conditions (at strain rates above 100 s^{-1}) can lie significantly above static stress-strain curves obtained at static strain rates (order 10^{-2} s^{-1} or less). Frequently in the case of static test results no specific strain rate is reported with the implication that rate (time)-independence prevails for static loading conditions. However static stress-strain curves can be obtained at loading rates which differ by several orders of magnitude, and rate-dependence may be present within the static strain-rate range. Indeed this has been demonstrated in the case of several metals [1-3] tested at room temperature. For AISI Type 304 Stainless Steel we have found significant room-temperature rate dependence manifested in loading-rate sensitivity of the yield and flow stresses at different static strain (stress) rates, and in creep and relaxation behavior. AISI Type 304 Stainless Steel exhibits low-yield strength, considerable work hardening, and high ductility. The Titanium Alloy used in this study has high-yield strength, normal work hardening, and considerably less ductility than AISI Type 304 Stainless Steel, and it is of interest to determine whether rate (time)-dependent behavior* occurs in this high-strength, low-ductility material. The room-temperature tests reported herein indicate significant rate-dependence in this Titanium Alloy very much akin to the rate-dependence observed in AISI Type 304 Stainless Steel. The tests consist of monotonic and cyclic loadings at static strain (stress)-rates differing by five orders of magnitude; and short-term relaxation tests. The results show that each loading rate has its own characteristic stress-strain curve and that rate-dependence is significant in static loading.

---

*Rate (time)-dependence encompasses loading rate sensitivity, creep and relaxation.

In viscoplasticity, some constitutive theories assume the existence of a quasistatic or equilibrium stress-strain curve [4-8] characteristic of the rate-independent portion of material response. In some cases [4-6] dynamic rate-dependence is recognized while rate-independence is assumed over the static strain-rate range, and the static (equilibrium) stress-strain curve is assumed to correspond to any static loading rate. The results of this study show that rate-sensitivity of yield and flow stresses remains significant in Titanium at low (static) loading rates, and that the equilibrium stress-strain curve used in constitutive theories should be determined at strain rates below 10^{-8} s^{-1}.

MATERIAL AND SPECIMENS

The Ti-7Al-2Cb-1Ta Alloy was donated by the Naval Research Laboratory and was identified by the NRL Code T89. Blanks of approximately 20×20×120 mm were cut from the top (Label T) and bottom (Label B) of a 3-in. (76.2 mm) thick plate. The longest side of the blanks was parallel to the direction of rolling. To equilibrate texture effects the blanks were subjected to a beta-anneal heat treatment of one-half hour at 2000°F in vacuum and subsequent cooling to room temperature in Helium at a rate approximating air cooling. Two different types of specimens shown in Figure 1 were machined from the heat-treated blanks. The specimens with the short-gage length were used for the cyclic experiments. A total of nine specimens were tested.

TESTING EQUIPMENT AND PROCEDURE

All specimens were tested in an MTS servocontrolled tension-torsion system with dual ramp function generator and the test results were recorded on an XY-recorder. Displacement was in all cases measured by an MTS clip-on extensometer clamped on the gage length and converted to engineering strain and strain rate using standard methods. In the following we refer to stress (strain)

control, creep, and relaxation. In actuality the load (displacement) is controlled. During creep the load is kept constant and during relaxation the displacement in the gage length is held fixed.

The clip-on extensometer together with the function generator and the servocontrolled system enable an accurate strain control which is not possible with conventional testing machines. By simply changing the command signal stress control can be achieved in the servocontrolled test system.

We have basically two sets of test histories, repeated loading and unloading with no negative stresses; and cyclic, completely reversed strain and load control using a sawtooth input signal. Each test history is piecewise linear in time and consists of constant stress or strain rate (ramp forcing function), of intervals of creep (constant load forcing function) or of relaxation intervals (constant displacement forcing function). All tests were executed at room temperature in air environment.

In some cases the extensometer was rezeroed before the test was restarted. If this is so, the prior history of deformation is noted on the graph. Engineering stresses based on the original cross section are used throughout this study.

TEST RESULTS

Behavior for Positive Stress

Influence of Loading Rate. Test results of three different specimens B2, B5 and T5 are depicted in Figure 2. Specimen B2 was loaded under stress control at 69 MPa s^{-1}. Repeated loadings and unloadings with strain rate changes were used in the tests with specimens B5 (full line) and T5 (dashed line).

The stress-strain behavior is initially linear with slope E on all loadings starting at points O, D, F and F_1. At stresses larger than 450 MPa

the effects of rate become noticeable and are significant in the plastic range*. Also the 0.2% yield strength is dependent on rate as seen in Figure 2.

Table I shows the variation of the 0.2% offset yield strength with loading rate. The difference between the yield strength at the slowest (2×10^{-8} s^{-1}) and fastest (1.7×10^{-3} s^{-1}) strain rate is 21% or 131 MPa. The yield strengths for three different specimens determined at the same strain rate (10^{-4} s^{-1}) differ at the most by 13 Mpa or 2%. We see that the scatter is not very large and that the influence of rate is very noticeable in the range of "static" strain rates.

The initial unloading behavior starting at points C, C_1, E and E_1 is not linear elastic. The slope is initially larger than the elastic modulus and continuously decreases as the stress decreases. At zero stress the unloading slope is less than the elastic modulus (see also Figure 3). The initial slope on reloading is equal to the modulus of elasticity and a small hysteretic loop develops as shown in Figure 2.

In the plastic range the stress-strain curves obtained at different strain rates are equidistant. The stress-strain diagram for specimen B2 obtained under stress control, however, shows a somewhat higher slope at a given strain level than the others.

For specimens B5 and T5 which were subjected to a different strain-rate history up to points F and F_1, respectively, the same strain rate of 10^{-5} s^{-1} was used in the final loading starting at F and F_1 and the two curves ultimately coincide within normal scatter.

Although specimens B5 and T5 underwent different strain and strain rate histories, their final stress-strain curves coincide when loaded with the same

*Plastic range is the region of the stress-strain curve in which the tangent modulus is small compared to the elastic modulus.

final strain rate. We conclude that the material forgets the prior history and that a strain rate history effect [9-11] is absent.

Figures 3 and 4 further demonstrate the effect of loading rate. In Figure 3 specimen T4 was first loaded and unloaded to zero stress at a strain rate of 10^{-5} s^{-1}, see curve (1) 0A. At point A a stress controlled loading was started right away. During one loading and unloading cycle the stress rate was kept constant; however, each new cycle (points B and C) was started with a tenfold reduced stress rate without changing the maximum stress, see curves (2), (3) and (4). It is evident that the stress rate has a significant effect on the ratchet-strain (distances AB, BC, CD) accumulated during one cycle. This ratchet-strain is caused by a "creep deformation" allowed by the stress control at stress levels approaching the maximum stress of the cycle*. This creeping is negligible at a stress rate of 21.7 MPa s^{-1} but becomes significant at 0.217 MPa s^{-1}. The stress controlled (2), (3), (4) and the strain controlled (1) unloading curves (4) and (1) display significant differences. The former show negative slopes which are absent for (1). For curve (2) the negative slope is not pronounced since not enough time is available for creep to develop during initial unloadings.

Figure 4 is intended to illustrate this effect of "creeping out" further. In this test only partial unloading is performed between σ_{max} and σ_{min} and the stress rate is varied by four orders of magnitude. It is important to note that the <u>maximum stress equals</u> the <u>maximum stress obtained during prior loading</u>. At $|\dot{\sigma}_1|$ ten loading-unloading cycles produce a small ratchet strain which is somewhat increased when the rate is decreased to $|\dot{\sigma}_2|$. (The dashed lines indicate a horizontal translation made for ease in interpreting the graph; they do not designate a ratchet strain.) A single cycle at $|\dot{\sigma}_3|$ produces almost as

*Such creeping motions are impossible in displacement control.

much ratchet strain as ten cycles at $|\dot{\sigma}_1|$. The two slowest rates produce significant ratchet strains. It should be noted that the last cycle took 51.42 hours to complete.

We see that stress rate has a significant effect on the ratchet strain accumulated in one cycle. It is of course very strongly dependent on stress level. Figure 4 implies that insignificant ratchet strain would have developed at a stress of 690 MPa at $|\dot{\sigma}_5|$, since the stress-strain curves corresponding to this loading rate are almost linear up to this stress level. Also the evidence in Figures 3 and 4 suggests that the ratchet strains measured at σ_{min} in Figure 4 are approximately equal to the ones measured at $\sigma = 0$.

Relaxation Behavior for Positive Stresses. The relaxation behavior of this material in the plastic range is shown in Figure 5 which depicts stress drops in 10 minutes and subsequent reloading at various strain rates. It is evident that the total stress drop and therefore the relaxation rate depends on the strain rate preceding the relaxation tests. The total stress drop is further independent of the strain at the start of the relaxation test. In other tests started at strains below the ones used in Figure 5 we found that the stress drop is also independent of the initial stress. The validity of these statements is demonstrated in Figure 6 where the stress drops in ten-minute relaxation of three different specimens are plotted versus total strain. We know from Figure 2 that a unique stress-strain curve is associated with a given strain rate. Consequently the stress drops shown in Figure 6 are also independent of the stress at the start of the relaxation test.

A crossplot of Figure 6 is shown in Figure 7 where we have added the stress drops for four- and one-minute relaxation time. Each point is the average for corresponding tests with specimens B4, B5 and T4.

The data in Figures 5 through 7 permit the following statement:

In the plastic range the stress drop in a given period of time depends only on the strain rate preceding the relaxation test. It is independent of the stress and strain at the start of the relaxation test.

The slopes of the reloading curves which commence after the ten-minute relaxation period in Figure 5 appear to depend on the strain rate. They decrease with decreasing strain rate. For the 10^{-7} s^{-1} curve a negative slope is obtained. It appears that the initial slope is close to the elastic modulus for 10^{-3} s^{-1} but less than the elastic modulus for strain rates below 10^{-3} s^{-1}.

Figure 8 reports the results of a separate test where the relaxation period was extended to twenty minutes followed by reloading at 5×10^{-5} s^{-1}. Figure 8 shows that the initial slope is slightly less than the elastic modulus. Other tests such as given in Figure 5 indicate that the exact value of this initial slope appears to depend on both the duration of the preceding relaxation test and the strain rate with which reloading is performed.

Figures 5 and 8 show that stress-strain curve eventually returns to a level characteristic of the particular strain rate. The material forgets the prior history if only relaxation and loading periods are involved. Instead of performing relaxation during loading, in the test corresponding to Figure 9 a relaxation period was introduced after partial unloading. It is evident that relaxation occurs at a reduced rate in the initial nearly linear section of the unloading stress-strain curve. Upon continued unloading the stress-strain curve does not return to the assumed original unloading curve (dashed in Figure 9). Rather it is displaced to the right.

Stress Change During Strain Rate Changes. Figures 2, 5 and 8 indicate that there exists at every strain a stress level characteristic of a given strain rate. Available data involving frequent relaxation periods and strain rate changes such as shown in Figure 5 were analyzed by determing steady stress values at a given strain for 10^{-6} and 10^{-3} s^{-1}. The results are shown in Figure 10. It is seen that the stress level differences are independent of strain and prior history as long as no cyclic loadings are involved.

Reversed Cyclic Loading

Strain Control. Completely reversed strain controlled cyclic loading was performed at a strain range of $\Delta\varepsilon$ = 1.6% (B1) and 2.4% (T1), respectively. Figure 11 demonstrates how the maximum tensile (σ_t) and compressive (σ_c) stresses change with cycles. The stress range ($\Delta\sigma = \sigma_t - \sigma_c$) is almost constant indicative of cyclically neutral behavior.

After the steady cyclic behavior was reached the effect of strain rate on the hysteresis loop was studied by changing the strain rate at suitable cycle intervals. At each strain rate two or three cycles were recorded before the next strain rate change was initiated. Both step-up and step-down changes in strain rate were performed.

After each change in strain rate a different hysteresis loop developed. The transition from one loop to the next was accomplished within less than .05% strain and was fully reversible, e.g., after a step-up test from 10^{-6} to 10^{-3} s^{-1} followed by a step-down test to 10^{-6} s^{-1} the two hysteresis loops for 10^{-6} s^{-1} coincided within experimental accuracy.

An increase in strain rate results in an increase in stress range and a decrease in the width of the loop at zero stress. The results are shown in Figure 12. For a change in three orders of magnitude in strain rate the corresponding stress range changes are 95 MPa or 7% and 125 MPa or 11% at

$\Delta\varepsilon$ = 1.6% and $\Delta\varepsilon$ = 2.4%, respectively. We also note that the two relationships $\Delta\sigma$ vs. strain rate are straight lines in the semilogarithmic plot. The line for $\Delta\sigma$ at $\Delta\varepsilon$ = 2.4% has a higher slope than the one for $\Delta\varepsilon$ = 1.6%. The plastic strain range (dashed lines in Figure 12) decreases with increasing strain rate.

Figure 13 illustrates how "inelasticity is distributed" around the hysteresis loop. The arrows with the numbers indicate the strains at which a two-minute relaxation test was introduced. At the end of these tests loading resumed at a strain rate of 10^{-3} s^{-1}. It is seen that no relaxation occurs in two minutes in the nearly straight portions of the loop and that relaxation increases gradually as the slope decreases. The initial slope at the commencement of each loading following relaxation is very close to the average slope during unloading and close to the modulus of elasticity. After the relaxation periods the stress-strain curve returns to the original hysteresis loop. The relaxation periods are forgotten. (The differences in the compression part of Figure 13 are probably due to continued cycle dependent changes in the loop. Figure 11 indicates that a complete steady state has not yet been reached at 30 cycles.)

Load (stress) control. Specimen B3 was used to perform stress-controlled loading with two-minute constant load creep periods ($\dot{\sigma}$=0) as indicated by the arrows on the right of Figure 14.

Starting from the origin the specimen was loaded to a maximum load and then unloaded to zero stress at point A, the end of section (1). Section (2) starts at A and ends at B where loading in compression and subsequent reloading in tension followed. Section (3) terminates at point C.

On loading ($\dot{\sigma} > 0$) creep develops gradually and in a nonlinear fashion. (Although the highest and lowest stress levels at which creep tests were

performed differ by less than a factor of two, the respective creep strains accumulated in two minutes differ by much more than a factor of two.) We also note that at the same stress level creep is less during unloading than during loading. This can be seen at the two highest stress levels of each of Sections (1), (2) and (3). Indeed no creep was found at all at the low stress levels during unloading. Also the creep strains during loading are at the same stress level different for sections (1), (2) and (3). Creep is least developed for section (2).

After the tests shown in Figure 14 the maximum stress was increased to $\pm$779 MPa and uninterrupted cycling continued for ten cycles at 1.5 MPa s^{-1}. Then after completion of one cycle the stress rate was consecutively decreased at zero stress going into compression and the changes in the hysteresis loop were observed, specifically the strains at zero stress. Figure 15 shows that the loop shifted towards positive strains (ε^* increases as the stress rate was decreased), and that both the width at zero load ($\Delta\varepsilon_{pl}$) and the total width ($\Delta\varepsilon_{tot}$) increased with decreasing rate. We also note that $\Delta\varepsilon_{pl}$ increases much faster than $\Delta\varepsilon_{tot}$.

The movement of the hysteretic loop to the right is probably due to a higher maximum true stress in tension than in compression (We use load control.). The movement is permanent. An increase of stress rate will narrow the loop; it will, however, continue to move towards positive strains. The original position of the loop, in contrast to strain cycling, will not be obtained when the stress rate returns to the same value after an excursion to low or high stress rates.

DISCUSSION

The results of this study show clearly that the inelastic deformation of this material is rate-dependent. The rate-dependence is basically logarithmic; the loading rates must be changed by an order of magnitude to get a significant change in the stress-strain behavior.

Both the elastic and inelastic behavior of this material is very consistent and very well reproducible. The modulus of elasticity (the slope at the stress-strain origin) for example was determined on nine specimens to be 117 GPa $\pm$ 1 GPa. It was independent of loading rate or gage length of the specimen.

From the results of this study a number of important qualitative conclusions regarding constitutive equation development can be obtained.

No Strain-Rate History Effect

The results shown in Figures 2, 5, 10 and others demonstrate that prior history can be "forgotten." A unique stress-strain curve is obtained for a given strain rate and positive stresses irrespective of prior history. We do not observe a strain rate history effect [9-11]. These results are in agreement with our findings for AISI Type 304 Stainless Steel [1,2] but are at variance with results obtained in dynamic plasticity [9-11] where strain rates in excess of 10^{-1} s^{-1} are involved.

The materials used in dynamic plasticity are different from the ones used by us. This fact could explain the difference in the findings. However, a very important difference is also in the experimental equipment. The servocontrolled testing machine insures that the strain rate is always maintained at the specified value. Such assurance is not available in dynamic plasticity experiments.

Inelasticity is Rate-Dependent

Inelasticity manifests itself through loading rate dependence, creep and

relaxation (Figures 2-5, 13 and 14). Moreover it is shown in Figure 5 that an increase in loading rate causes an increase in the relaxation drop in a given time period. This result is confirmed by the other results shown in Figures 6 and 7.

The results further suggest that the source of inelasticity is the loading rate. A low loading rate causes reduced relaxation. Relaxation effects are pronounced when loading rates are high. The same qualitative relationships were found for AISI Type 304 Stainless Steel [1,2]. We suggest that relaxation will be absent for extremely slow loading.

Relaxation and Strain Rate-Stress Change Behavior

Figures 5-7 show that relaxation behavior depends only on the strain rate preceding the relaxation test. Figures 5 and 6 also demonstrate that this property is independent of the prior history.

Figures 2 and 5 further suggest that a stress-strain curve is characteristic of a given strain rate irrespective of the prior history. This property is verified in Figure 10. The data are from two specimens which underwent repeated relaxation and strain-rate change tests. (For clarity only the curves pertinent to 10^{-3} and 10^{-6} s^{-1} are shown.)

A dependence on prior history is, however, shown by the data obtained in Figure 10 with specimen T1 which underwent prior strain cycling at $\Delta\varepsilon = 2.4\%$. After about 60 cycles the specimen was unloaded from tension to zero load. A regular tensile test with strain rate changes was then started.

Figure 10 then shows that the absolute stress level of the cycled specimen is less than for the zero-to-tension loaded specimens T4 and T5. Some cyclic softening (see Figure 11) has occurred. Table II, however, demonstrates that the stress change before and after cyclic loading is equal within the accuracy of the extrapolation used in getting the data.

The inelastic behavior of this high-strength Ti-alloy is that of a nonlinear viscoelastic material as long as only zero-to-tension loading is considered. Prior loading history in strain-rate change and relaxation is forgotten after an initial transient period.

Cyclic loading changes the stress level characteristic of a given strain rate. The strain rate-stress change behavior remains unaltered.

In the experiments on AISI Type 304 Stainless Steel [1] which undergoes considerable cyclic hardening both the stress level and the stress level difference were altered. For the Ti-alloy only the stress level is affected by cyclic loading.

Unloading and Reloading Behavior

Figures 2-5, 9, 13 and 14 show that inelastic behavior is observed at and below the prior maximum stress level of a specimen. This is especially true for Figures 9, 13 and 14. Figures 13 and 14 also indicate that inelasticity develops differently in loading and unloading.

In the unloading leg, beginning at some stress level below the maximum stress, a nearly rate-independent, linear behavior is observed which in this material extends to and beyond the zero stress axis. It appears therefore that during unloading a region of almost elastic behavior is found which is very close to the behavior obtained at the origin upon initial loading.

The observed behavior contradicts viscoplasticity theories which assume that the yield surface extends with the stress point and that elasticity prevails inside the yield surface.

Also the observed creep behavior in Figure 14 is at variance with creep theories which assume that creep rate depends only on creep strain and stress.

Similar observations have been made for AISI Type 304 Stainless Steel [1,2]. This material also exhibits mechanical behavior at variance with the previously

mentioned viscoplasticity and creep theories.

The type of control influences the unloading behavior considerably. When a low stress rate is used creeping out is observed during unloading, which can be considerable (Figures 4 and 3). No such creep effect is possible in strain control. Constitutive theories should account for this bias between stress and strain control.

Comparison with Others

Historical remarks. The test results do not support the notion of rate (time)-independent behavior postulated in plasticity theories. It is interesting to observe that room-temperature rate-dependence of metals was reported by Ludwik [17,18] in 1909. Prandtl [19] in a 1928 paper considers rate-dependence in his theory which postulates that the applied load is proportional to the logarithm of the deformation rate (Eqs. (17) and (18) in [19]). Ludwik's observations [17,18] were not used by v. Mises [20] when he established his rate-independent theory in 1913. His notion of rate-independence is still widely accepted.

The present results are qualitatively in accordance with [17,18,19] but show in addition that rate-dependence, creep and relaxation are in interdependent.

Own experiments on AISI Type 304 Stainless Steel. Although AISI Type 304 SS is low-strength, high-ductility material, its inelastic behavior [1,2] is quantitatively the same as this high-strength, low-ductility Ti-alloy*. Although the stress levels are quite different in the two cases, the relaxation, the strain rate-stress change behavior and the unloading behavior are qualitatively the same. These findings suggest that the viscoplastic model based on total strain and overstress [12-16] is capable of qualitatively reproducing the behavior observed herein.

---

*All tests with the Ti-alloy were terminated at strains of approximately 7%. Small cracks were usually observed around this strain.

ACKNOWLEDGMENT

This research was supported by the National Science Foundation and the Office of Naval Research. The heat treated Ti-blanks were donated by the Naval Research Laboratory through Dr. T. A. Crooker. Helpful comments of Drs. Y. Asada and E. P. Cernocky are appreciated. Mr. V. Kallianpur helped in the preparation of the manuscript.

REFERENCES

1. Krempl, E., An Experimental Study of Room-Temperature Rate-Sensitivity, Creep and Relaxation of AISI Type 304 Stainless Steel, J. Mech. Phys. Solids, 27, (1979).

2. Kujawski, D., V. Kallianpur and E. Krempl, Uniaxial Creep and Relaxation of AISI Type 304 Stainless Steel at Room Temperature, RPI Report CS 79-4 (August 1979).

3. Baron, H. G., Stress-Strain Curves of Some Metals and Alloys, at Low Temperatures and High Rates of Strain, J. Iron and Steel Inst., 354-365 (1956).

4. Malvern, L. E., The Propagation of Longitudinal Waves of Plastic Deformation in a Bar of Material Exhibiting a Strain Rate Effect, Trans. ASME, 18E, 203-208 (1951).

5. Perzyna, P., The Constitutive Equation for Rate Sensitive Plastic Materials, Quart. of Appl. Math., 20, 321-332 (1963).

6. Eisenberg, M. A., C. W. Lee and A. Phillips, Observations on the Theoretical and Experimental Foundations of Thermoplasticity, Int. J. Solids and Structures, 13, 1239-1255 (1977).

7. Cristescu, N., A Procedure for Determining the Constitutive Equations for Materials Exhibiting Both Time-Dependent and Time-Independent Plasticity, Int. J. Solids and Structures, 8, 511-530 (1972).

8. Cristescu, N., Dynamic Plasticity, North Holland (1967).

9. Klepaczko, J., Thermally Activated Flow and Strain Rate History Effect for Some Polycrystalline fcc Metals, J. Mat. Sci. Eng., 18, 121-135 (1975).

10. Nicholas, T., Strain-Rate and Strain-Rate-History Effects in Several Metals in Torsion, Experimental Mechanics, 11, 370-374 (1971).

11. Campbell, J. D. and T. L. Briggs, Strain-Rate History Effects in Polycrystalline Molybdenum and Niobium, J. Less Common Metals, 40, 235-250 (1975).

12. Cernocky, E. P. and E. Krempl, A Nonlinear Uniaxial Integral Constitutive Equation Incorporating Rate Effects, Creep, and Relaxation, to appear in Int. J. Nonlinear Mechanics (1979).

13. Cernocky, E. P. and E. Krempl, A Theory of Viscoplasticity Based on Infinitesimal Total Strain, to appear Acta Mechanica.

14. Liu, M.C.M. and E. Krempl, A Uniaxial Viscoplastic Model Based on Total Strain and Overstress, J. Mech. Phys. Solids, 27, (1979).

15. Cernocky, E. P. and E. Krempl, A Theory of Thermoviscoplasticity Based on Infinitesimal Total Strain, to appear Int. J. of Solids and Structures.

16. Cernocky, E. P. and E. Krempl, A Theory of Thermoviscoplasticity for Uniaxial Mechanical and Thermal Loading, to appear J. de Méchanique Appliquée.

17. Ludwik, P., Elemente der Technologischen Mechanik, Berlin (1909).

18. Ludwik, P., Über den Einfluss der Deformationsgeschwindigkeit bei bleibenden Deformationen mit besonderer Berücksichtigung der Nachwirkungserscheinungen, Physikalische Zeitschrift 10, 411-417 (1909).

19. Prandtl, L., Ein Gedankenmodell zur kinetischen Theorie der festen Körper, ZAMM 8, 85-106 (1928).

20. von Mises, R., Mechanik der festen Körper im plastisch deformablen Zustand, Göttinger Nachrichten, math-phys. Klasse, 582-592 (1913).

TABLE I

RATE-DEPENDENCE OF 0.2% OFFSET YIELD STRENGTH σ_y

Specimen No.	$\dot{\epsilon}$ s^{-1}	$\dot{\sigma}$ MPa s^{-1}	σ_y MPa
B1	10^{-4}		738
B2		69	764
B4	10^{-4}		730
B5	1.7×10^{-3}		763
T1	10^{-4}		725
T4	10^{-5}		675
T5	2×10^{-8}		632

TABLE II

STRAIN RATE CHANGE - STRESS CHANGE BEHAVIOR

Strain Rate Change From s^{-1}	To	Corresponding Stress Change* MPa Zero-to-Tension Loading Specimen T4	After Cyclic** Loading Specimen T1
10^{-3}	10^{-4}	24.9	24.8
10^{-3}	10^{-5}	45.8	47.6
10^{-3}	10^{-6}	65.6	63.7
10^{-3}	10^{-7}	82.1	79.7
10^{-4}	10^{-5}	20.9	19.5
10^{-6}	10^{-6}	40.8	37.2
10^{-5}	10^{-6}	19.4	17.7

* Stress change is obtained from the xy-records by an extrapolation of the respective stress-strain diagrams. An example of such an extrapolation is given in Figure 5.

** About 60 cycles at $\pm$ 1.2%.

FIGURE CAPTIONS

Figure 1 - Specimens Used in This Study

Figure 2 - The Effect of Loading Rate and Type of Control on the Stress-Strain Diagram of Three Different Specimens.
No strain-rate history effect is observed.

Figure 3 - Effect of Type of Loading and Loading Rate on Unloading Behavior.
The amount of ratchet strain (strain accumulation) increases with a decrease in stress rate.

Figure 4 - Effect of Stress Rate on Ratchet Strain for Partial Unloading.
The two dashed horizontal lines indicate a translation made for ease in interpreting the graph. They have no physical significance.

Figure 5 - Relaxation and Strain-Rate Change-Stress Change Behavior.
After completion of a ten-minute relaxation test loading was continued at the indicated strain rate. The distances a are examples of the stress changes reported in Table II.

Figure 6 - Stress Drops during Ten-Minute Relaxation Tests Obtained with Specimens B4, B5, T4.
Although each specimen was subjected to a different history, the relaxation behavior depends only on strain rate prior to the start of the relaxation test.

Figure 7 - Stress Drops Corresponding to Various Relaxation Times vs. Strain Rate Prior to Start of Relaxation Test.
Points are average values of specimens B4, B5, T4.

Figure 8 - Relaxation Test (20 min) and Subsequent Reloading.
The slope upon subsequent reloading is slightly less than the elastic modulus.

Figure 9 - Relaxation Periods of 20 Min. during Loading (a) and Unloading Below the Maximum Stress Level (b).
The relaxation period (b) causes a displacement of the stress-strain curve to the right.

Figure 10 - Stress Values Characteristic of a Given Strain Rate vs. Strain for Three Different Specimens.
Each specimen was subjected to frequent relaxation and strain rate changes as demonstrated in Figure 5. Although the stress levels are different for the cyclically preloaded specimen the stress level differences for the same strain rates are equal. See also Table II.

Figure 11 - Maximum Tensile Stress σ_t and Maximum Compressive Stress σ_c vs. Cycles.
The stress range ($\sigma_t - \sigma_c$) changes very little indicative of cyclically neutral behavior.

FIGURE CAPTIONS (continued)

Figure 12 - The Influence of Strain Rate on the Stress Range and the Width of the Hysteresis Loop at Zero Stress for a Strain Range of 2.4 and 1.6%.
Transitions from loops obtained at various strain rates are reversible.

Figure 13 - Strain-Controlled Test at $\Delta\varepsilon = 2.4\%$ with Two-Minute Relaxation Periods Commencing at Each Arrow and Subsequent Loading at $|\dot{\varepsilon}| = 10^{-3}\ s^{-1}$.
Almost elastic behavior is observed in the nearly straight portions of the loop.

Figure 14 - Load Controlled Loading.
At the stress levels corresponding to the arrows on the right two-minute creep periods are introduced. Creep develops gradually and is more pronounced on loading than on unloading.

Figure 15 - Load Controlled Loading, Continuation of Test in Figure 14.
The influence of loading rate on the total strain range, the plastic strain range and the strain reached during unloading from tension. The movement of the loop towards increasing strain is permanent.

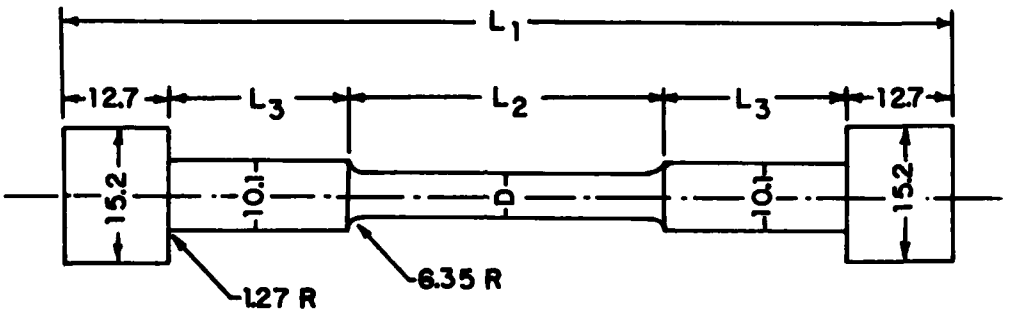

SPECIMEN	L_1	L_2	L_3	D
B1, B3, T1, T3	121.92	20.32	38.1	6.35
B2, B4, B5, T4, T5	120.65	44.45	25.4	7.62

ALL DIMENSIONS IN MILLIMETERS

Figure 1

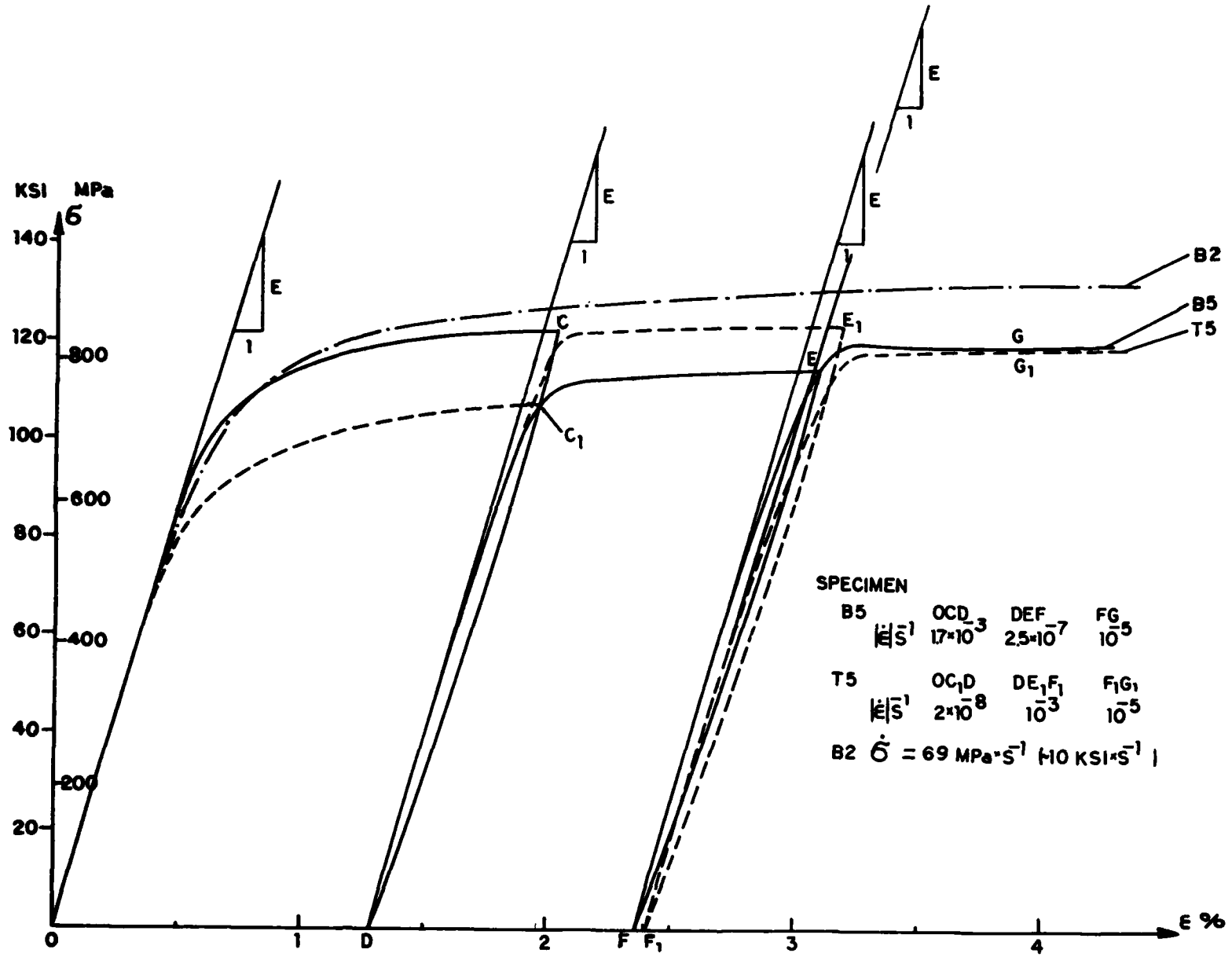
KSI MPa
σ
140
120
100
80
60
40
20
800
600
400
200
E
1
C
C1
E1
G
G1
B2
B5
T5
0
1
D
2
F
F1
3
4
ε %
SPECIMEN
B5 OCD DEF FG
|ε̇|s⁻¹ 1.7×10⁻³ 2.5×10⁻⁷ 10⁻⁵
T5 OC1D DE1F1 F1G1
|ε̇|s⁻¹ 2×10⁻⁸ 10⁻³ 10⁻⁵
B2 σ̇ = 69 MPa·s⁻¹ (10 KSI·s⁻¹)

Figure 2

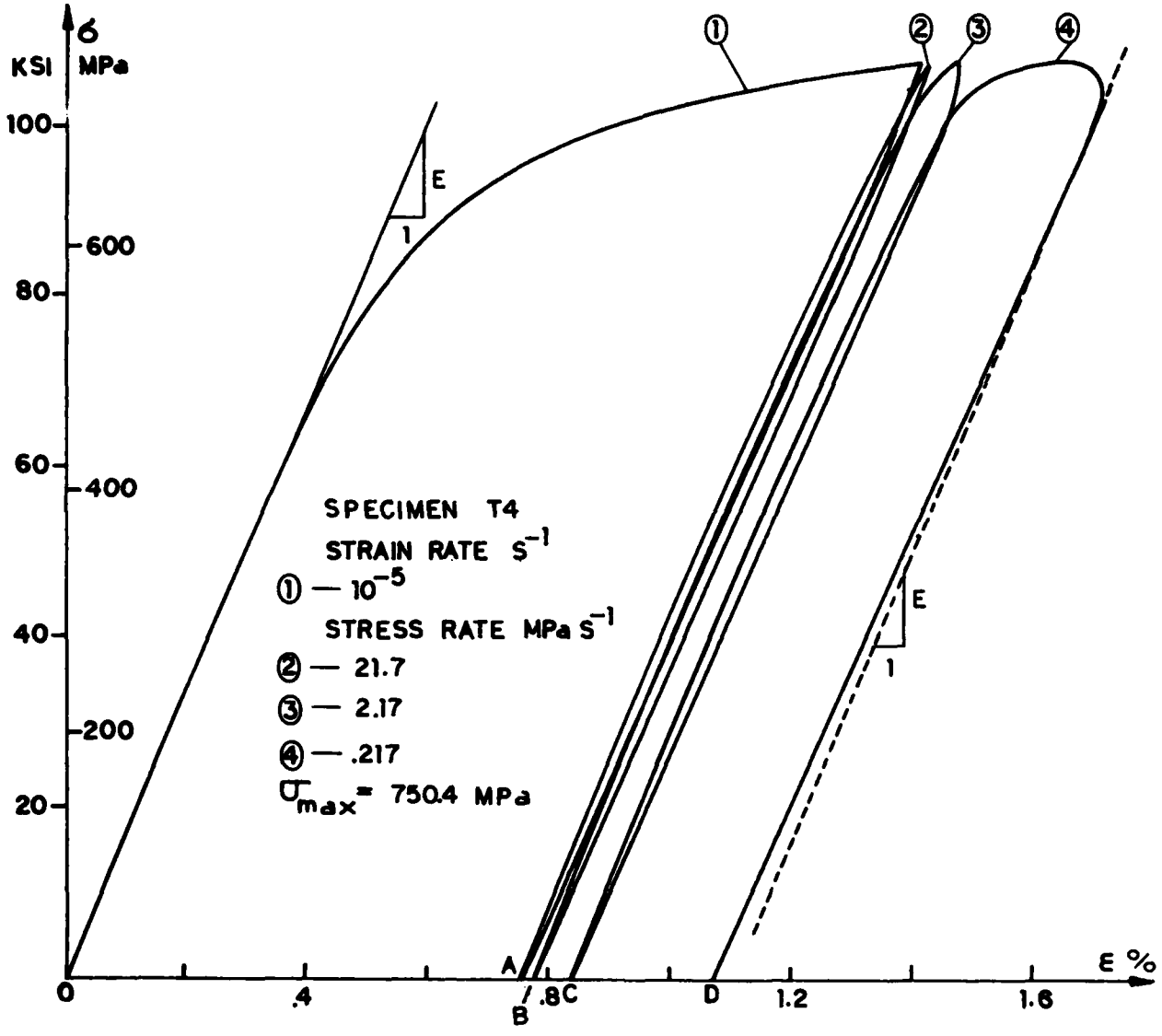
σ
KSI
MPa
100
600
80
60
400
40
200
20
E
1
SPECIMEN T4
STRAIN RATE S^{-1}
① — 10^{-5}
STRESS RATE MPa S^{-1}
② — 21.7
③ — 2.17
④ — .217
σ_{max} = 750.4 MPa
①
②
③
④
A
B
C
D
0
.4
.8
1.2
1.6
ε %

Figure 3

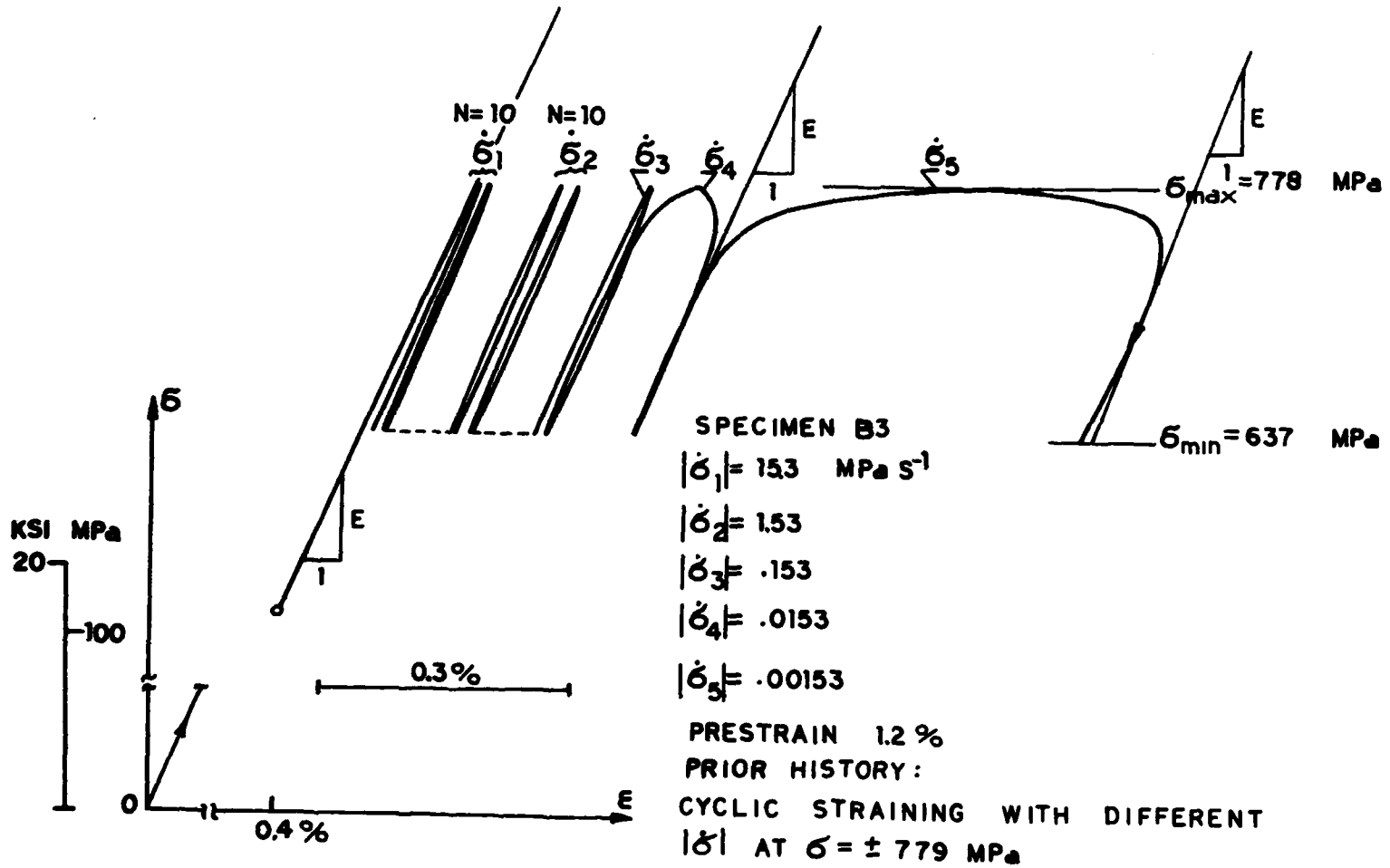
N= 10
N= 10
$\dot{\sigma}_1$
$\dot{\sigma}_2$
$\dot{\sigma}_3$
$\dot{\sigma}_4$
$\dot{\sigma}_5$
E
1
σ_{max} = 778 MPa
σ_{min} = 637 MPa
σ
KSI MPa
20
100
0
0.3%
0.4%
ε
SPECIMEN B3
$|\dot{\sigma}_1|$ = 153 MPa S^{-1}
$|\dot{\sigma}_2|$ = 1.53
$|\dot{\sigma}_3|$ = .153
$|\dot{\sigma}_4|$ = .0153
$|\dot{\sigma}_5|$ = .00153
PRESTRAIN 1.2 %
PRIOR HISTORY:
CYCLIC STRAINING WITH DIFFERENT
$|\dot{\sigma}|$ AT σ = ± 779 MPa

Figure 4

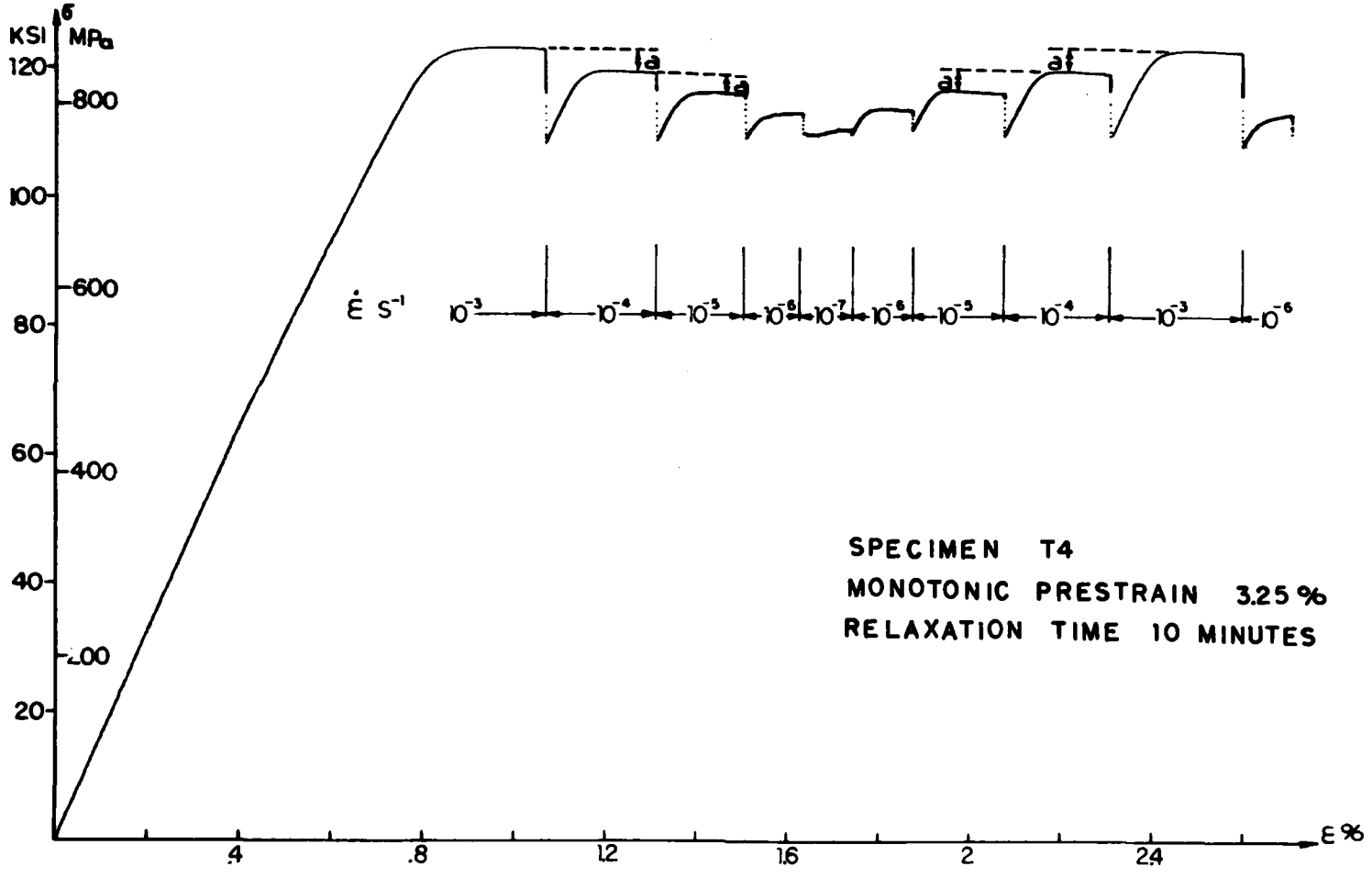
σ
KSI
MPa
120
800
100
600
80
60
400
40
200
20
ta
ta
af
af
Ė S⁻¹
10⁻³
10⁻⁴
10⁻⁵
10⁻⁶
10⁻⁷
10⁻⁶
10⁻⁵
10⁻⁴
10⁻³
10⁻⁶
SPECIMEN T4
MONOTONIC PRESTRAIN 3.25 %
RELAXATION TIME 10 MINUTES
.4
.8
1.2
1.6
2
2.4
ε %

Figure 5

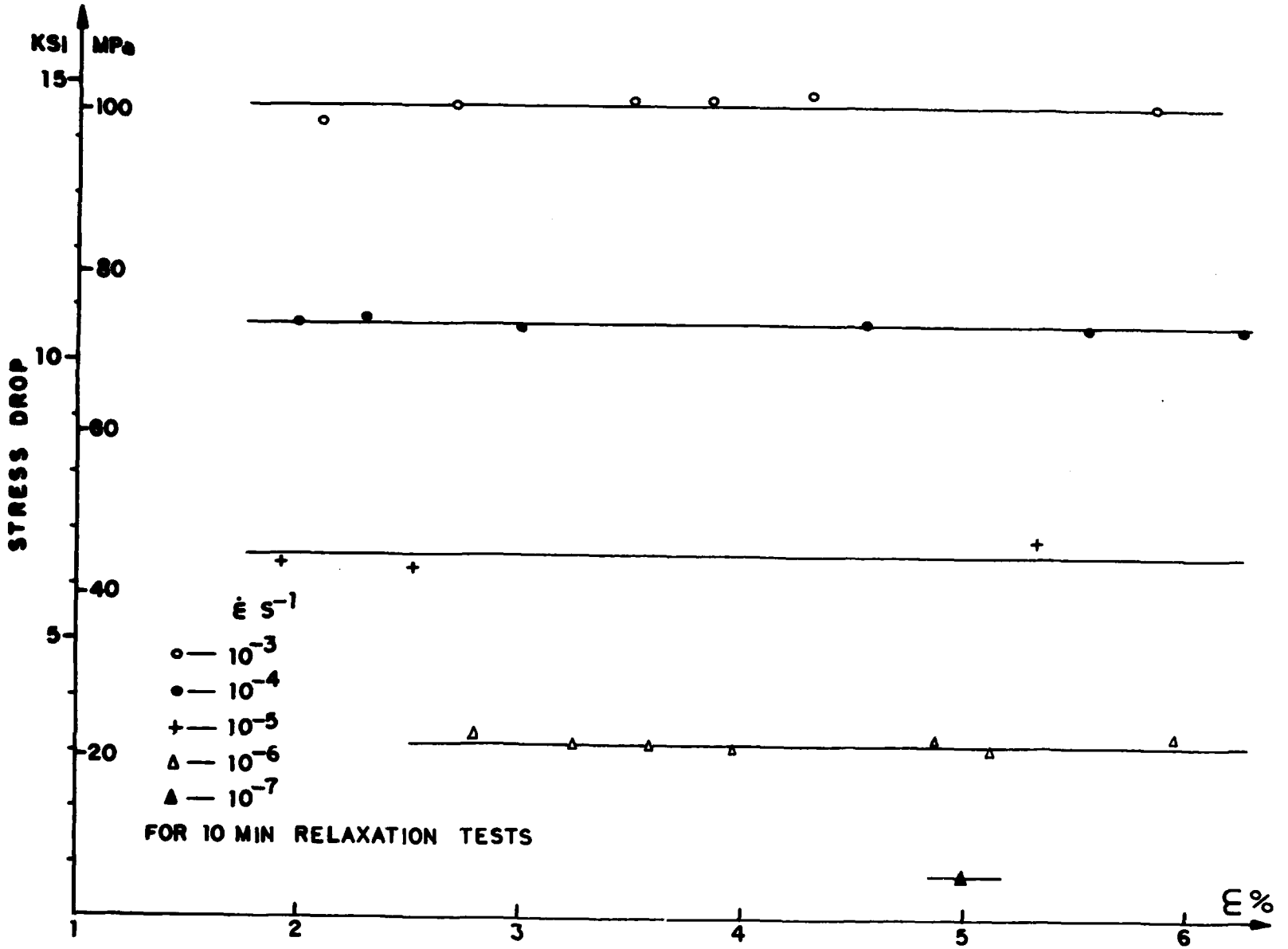
KSI
MPa
15
100
80
10
60
40
5
20
STRESS DROP
$\dot{E}$ S^{-1}
o — 10^{-3}
• — 10^{-4}
+ — 10^{-5}
Δ — 10^{-6}
▲ — 10^{-7}
FOR 10 MIN RELAXATION TESTS
1
2
3
4
5
6
ε%

Figure 6

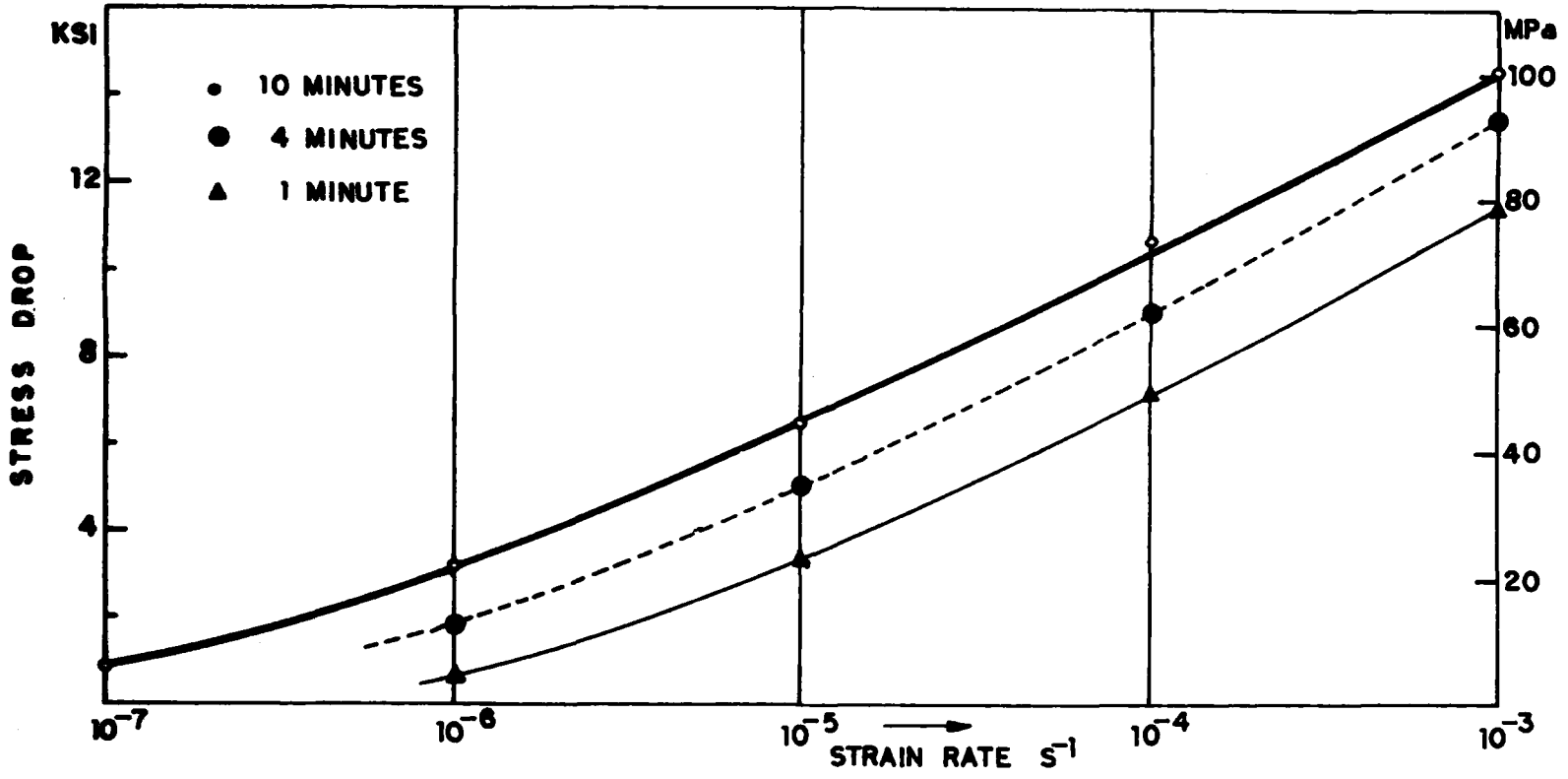
KSI
MPa
10 MINUTES
4 MINUTES
1 MINUTE
STRESS DROP
12
8
4
100
80
60
40
20
10^{-7}
10^{-6}
10^{-5}
10^{-4}
10^{-3}
STRAIN RATE S^{-1}

Figure 7

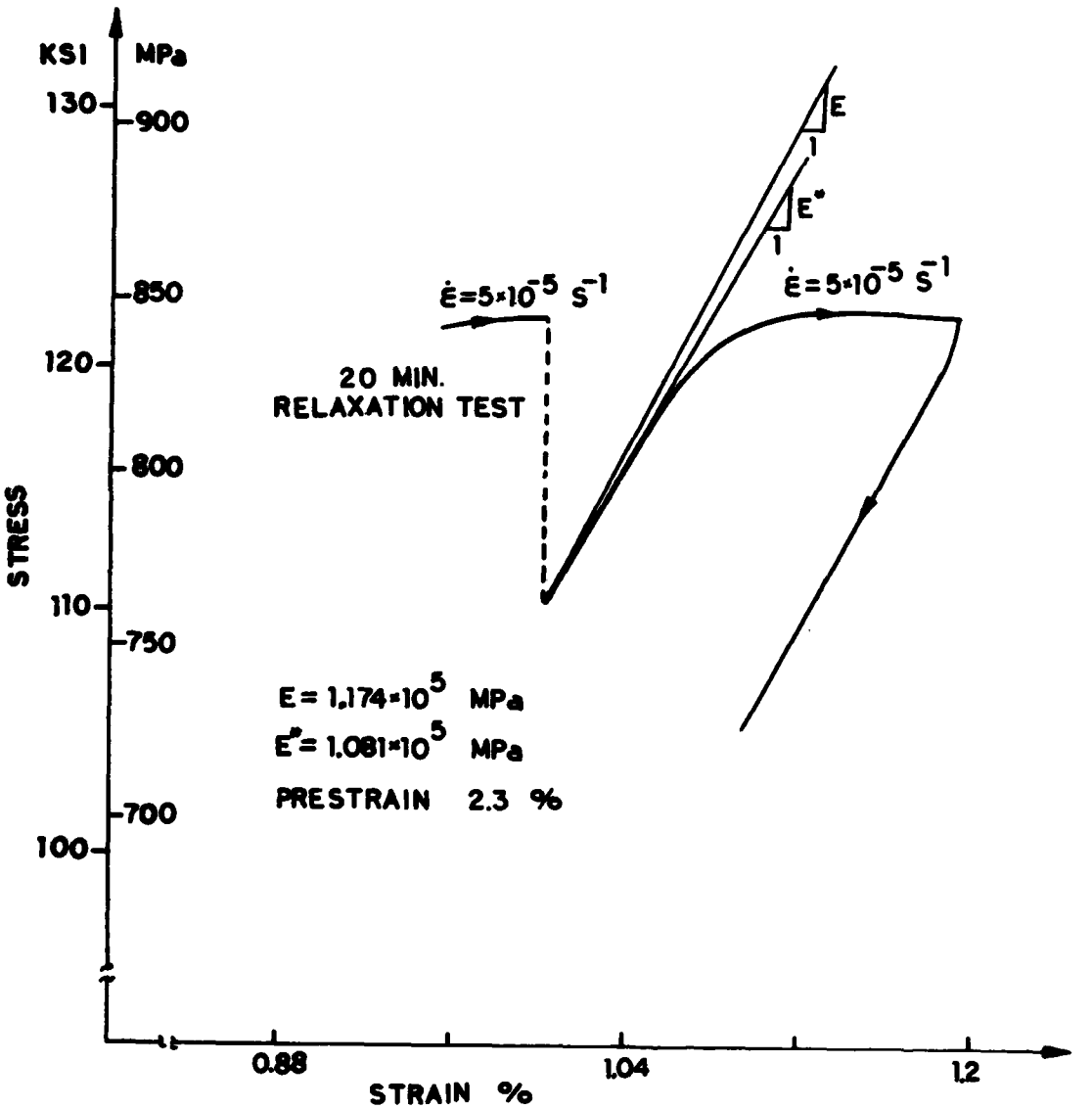
KSI
MPa
130
900
850
120
800
110
750
700
100
STRESS
$\dot{E}=5\times10^{-5}\ s^{-1}$
20 MIN.
RELAXATION TEST
E
1
E*
1
$\dot{E}=5\times10^{-5}\ s^{-1}$
$E = 1.174\times10^{5}$ MPa
$E^{*} = 1.081\times10^{5}$ MPa
PRESTRAIN 2.3 %
0.88
1.04
1.2
STRAIN %

Figure 8

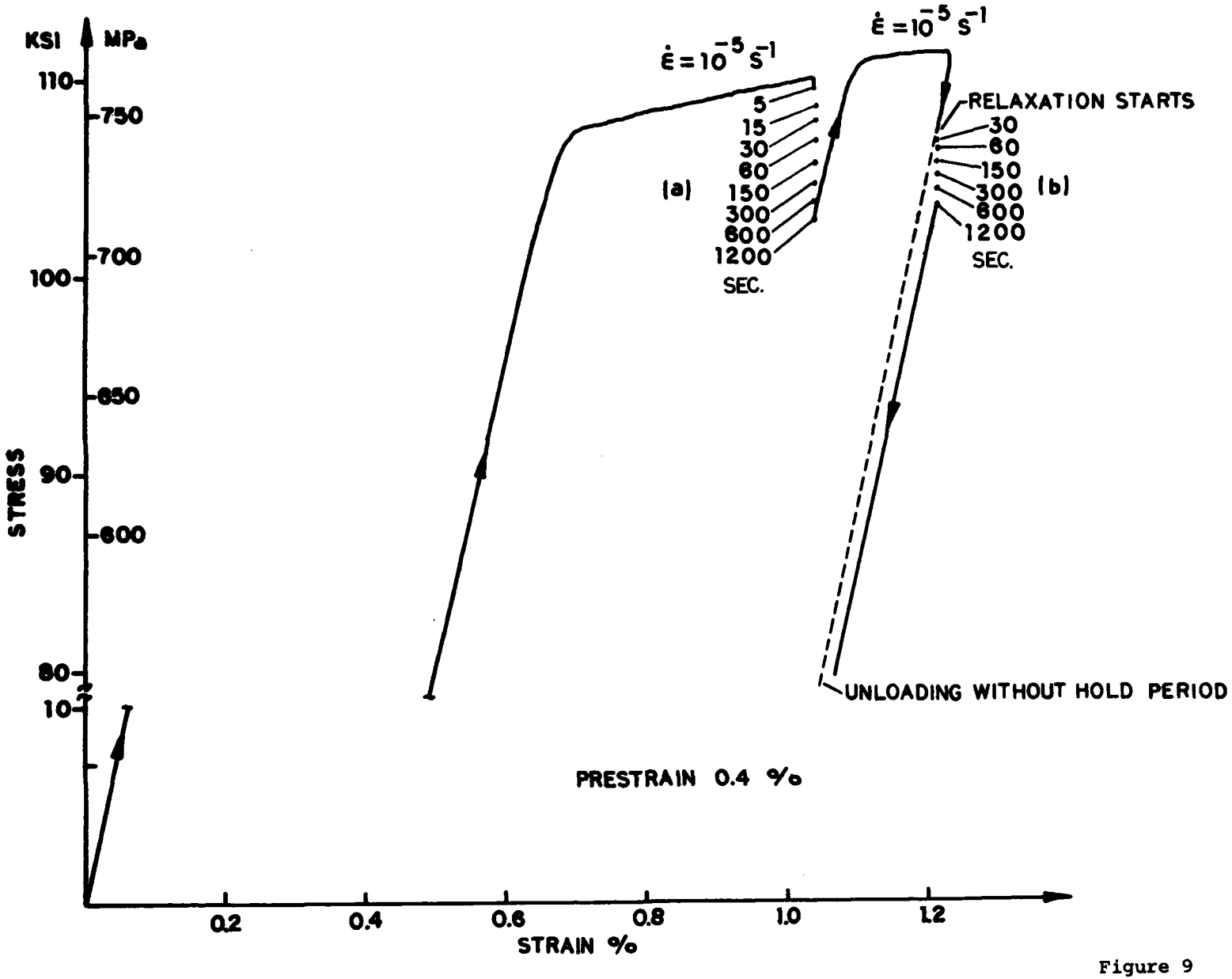
KSI
MPa
110
750
700
100
650
90
600
80
10
STRESS
$\dot{\epsilon} = 10^{-5}\ s^{-1}$
$\dot{\epsilon} = 10^{-5}\ s^{-1}$
5
15
30
60
150
300
600
1200
SEC.
(a)
RELAXATION STARTS
30
60
150
300
600
1200
SEC.
(b)
UNLOADING WITHOUT HOLD PERIOD
PRESTRAIN 0.4 %
0.2
0.4
0.6
0.8
1.0
1.2
STRAIN %

Figure 9

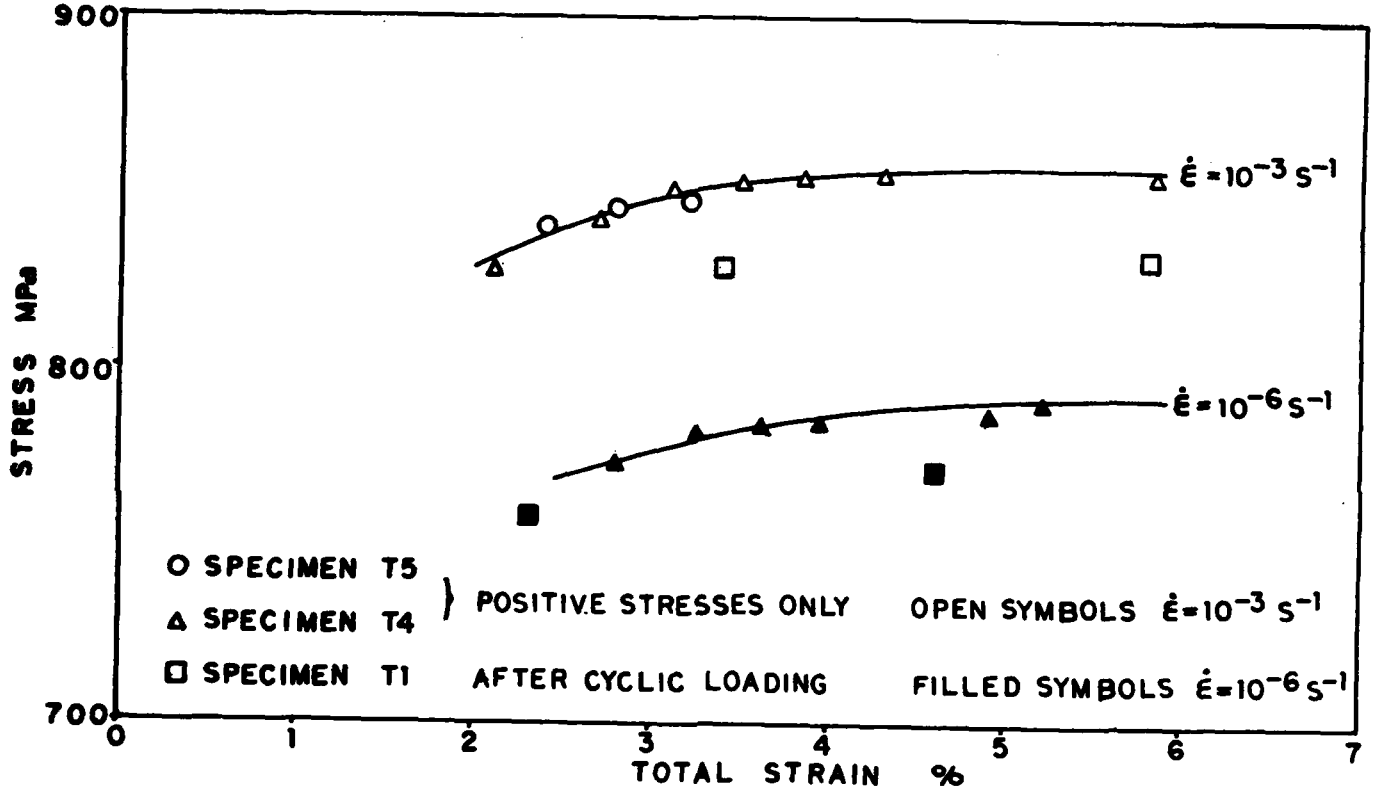
900
800
700
STRESS MPa
0
1
2
3
4
5
6
7
TOTAL STRAIN %
$\dot{\varepsilon}=10^{-3}\,s^{-1}$
$\dot{\varepsilon}=10^{-6}\,s^{-1}$
O SPECIMEN T5
Δ SPECIMEN T4
□ SPECIMEN T1
POSITIVE STRESSES ONLY
AFTER CYCLIC LOADING
OPEN SYMBOLS $\dot{\varepsilon}=10^{-3}\,s^{-1}$
FILLED SYMBOLS $\dot{\varepsilon}=10^{-6}\,s^{-1}$

Figure 10

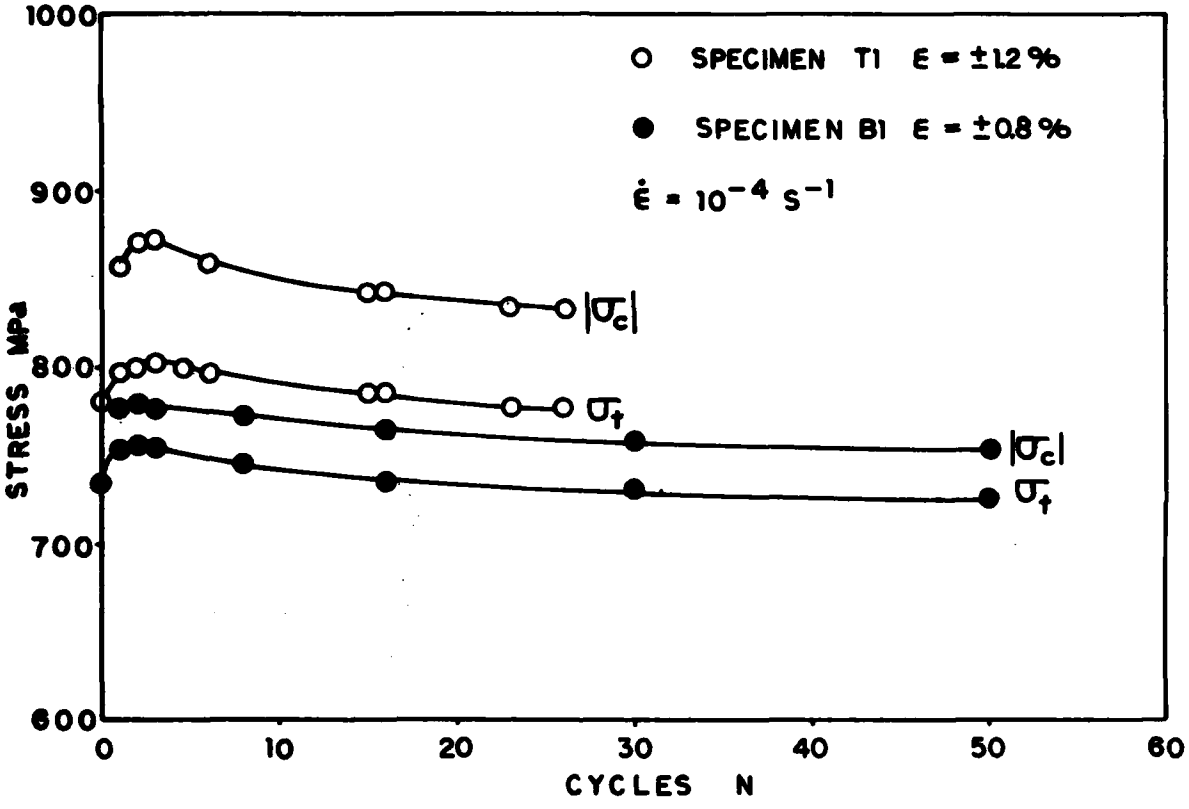
1000
900
800
700
600
STRESS MPa
0
10
20
30
40
50
60
CYCLES N
O SPECIMEN T1 ε = ±1.2 %
● SPECIMEN B1 ε = ±0.8 %
$\dot{\varepsilon} = 10^{-4}\ s^{-1}$
$|\sigma_c|$
σ_t
$|\sigma_c|$
σ_t

Figure 11

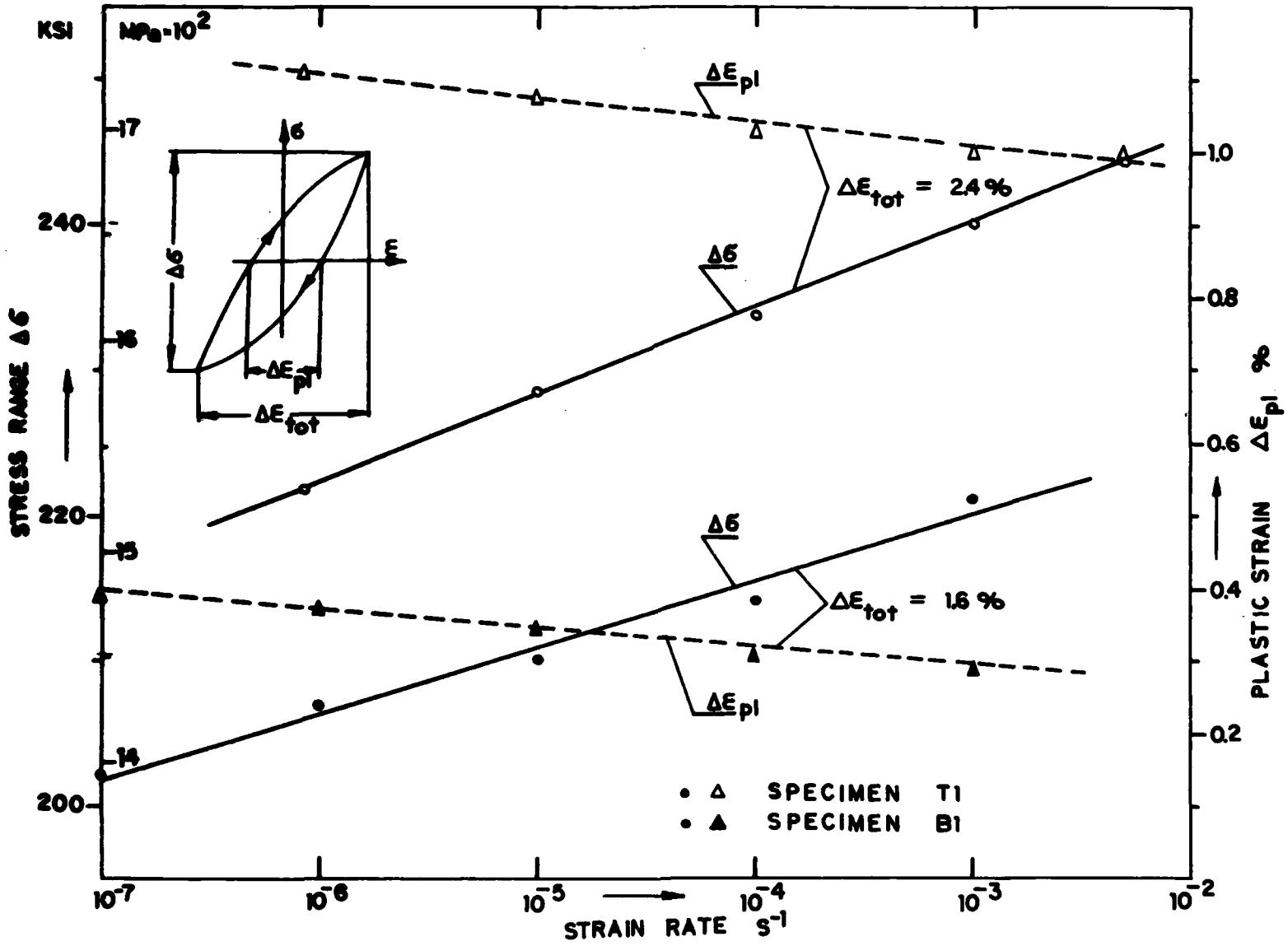
KSI
MPa·10²
17
240
16
220
15
14
200
STRESS RANGE Δσ
PLASTIC STRAIN Δε_pl %
1.0
0.8
0.6
0.4
0.2
Δε_pl
Δε_tot = 2.4 %
Δσ
Δε_tot = 1.6 %
Δσ
Δε_pl
σ
Δσ
ε
Δε_pl
Δε_tot
• △ SPECIMEN T1
• ▲ SPECIMEN B1
10⁻⁷
10⁻⁶
10⁻⁵
10⁻⁴
10⁻³
10⁻²
STRAIN RATE s⁻¹

Figure 12

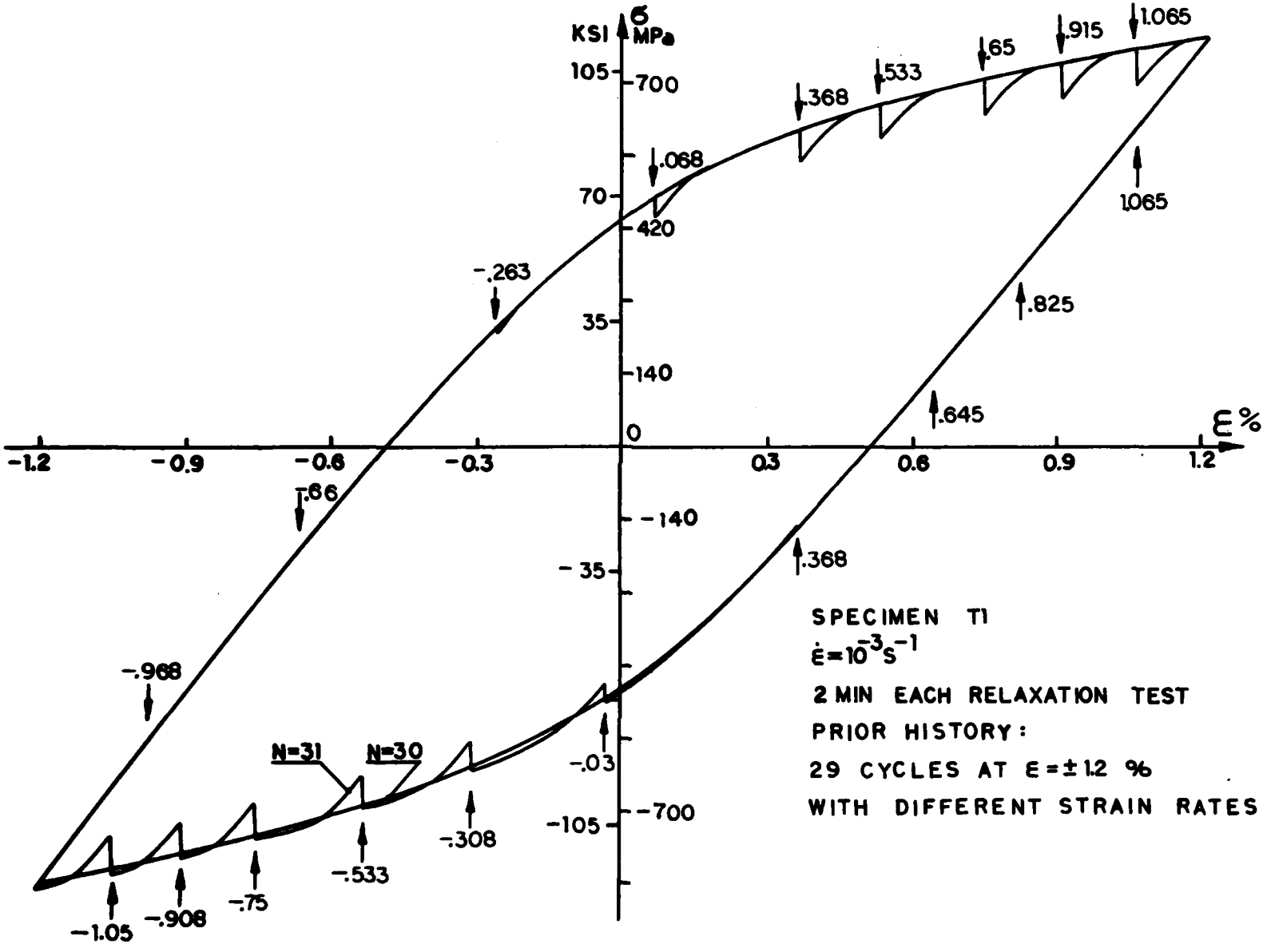
σ
KSI
MPa
105
700
70
420
35
140
0
-140
-35
-700
-105
ε %
-1.2
-0.9
-0.6
-0.3
0.3
0.6
0.9
1.2
.065
.368
.533
.915
1.065
.068
1.065
-.263
.825
.645
-.66
.368
-.968
N=31
N=30
-.03
-.308
-.533
-.75
-.908
-1.05
SPECIMEN T1
$\dot{\varepsilon}=10^{-3}s^{-1}$
2 MIN EACH RELAXATION TEST
PRIOR HISTORY:
29 CYCLES AT ε = ± 1.2 %
WITH DIFFERENT STRAIN RATES

Figure 13

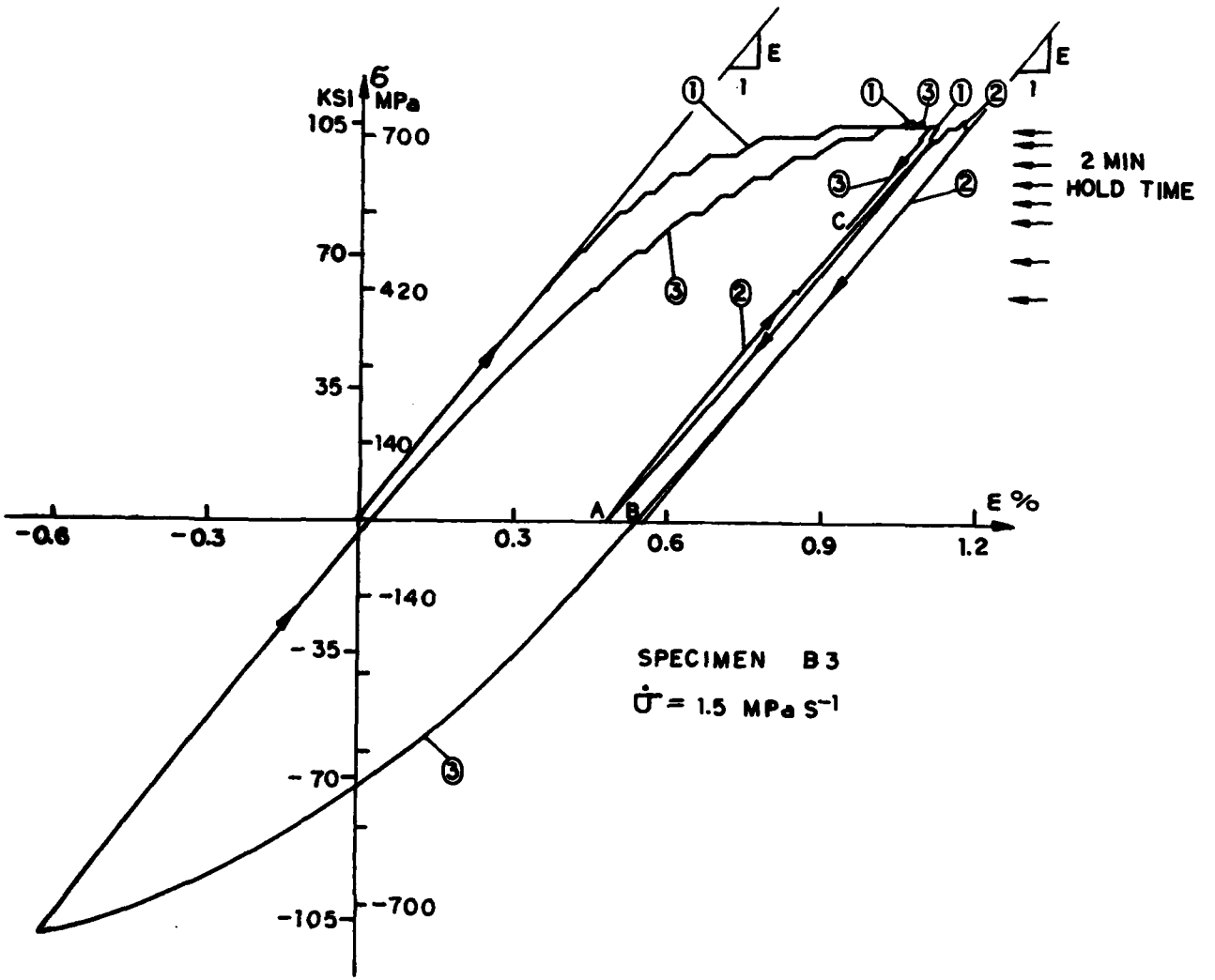
σ
KSI
MPa
105
700
70
420
35
140
-140
-35
-70
-105
-700
-0.6
-0.3
0.3
0.6
0.9
1.2
E %
A
B
C
E
1
2 MIN
HOLD TIME
SPECIMEN B3
σ̇ = 1.5 MPa S⁻¹

Figure 14

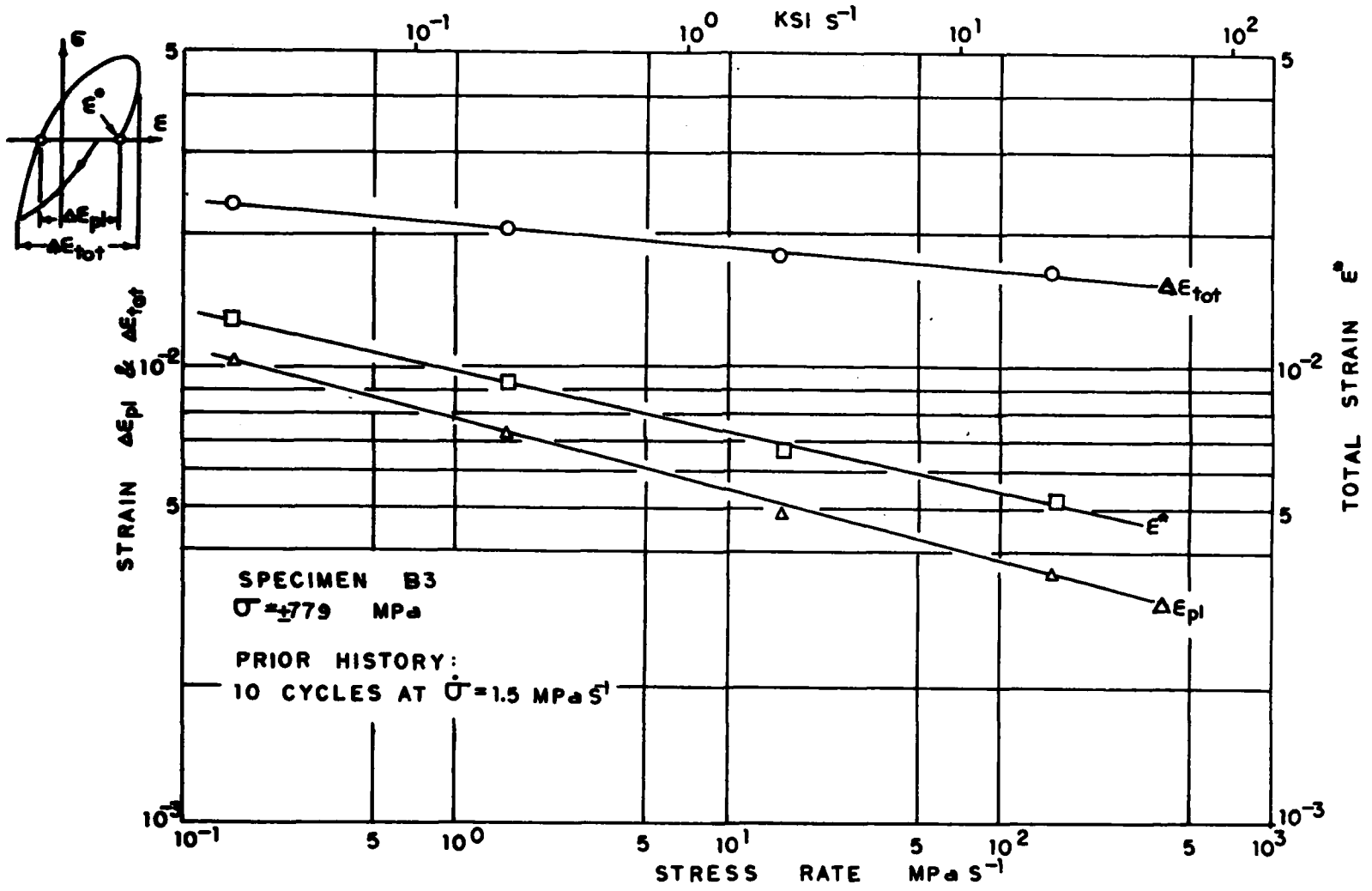
σ
ε*
ε
Δε_pl
Δε_tot
KSI S⁻¹
10⁻¹
10⁰
10¹
10²
STRAIN Δε_pl & Δε_tot
TOTAL STRAIN ε*
Δε_tot
ε*
Δε_pl
SPECIMEN B3
σ̇ = ±779 MPa
PRIOR HISTORY:
10 CYCLES AT σ̇ = 1.5 MPa S⁻¹
STRESS RATE MPa S⁻¹
10⁻¹
10⁰
10¹
10²
10³
10⁻²
10⁻³
5

Figure 15

SECURITY CLASSIFICATION OF THIS PAGE *(When Data Entered)*

REPORT DOCUMENTATION PAGE		READ INSTRUCTIONS BEFORE COMPLETING FORM
1. REPORT NUMBER RPI CS 79-5 ✓	2. GOVT ACCESSION NO.	3. RECIPIENT'S CATALOG NUMBER
4. TITLE *(and Subtitle)* THE RATE (TIME)-DEPENDENT BEHAVIOR OF Ti-7Al-2Cb-1Ta TITANIUM ALLOY AT ROOM TEMPERATURE UNDER QUASISTATIC MONOTONIC AND CYCLIC LOADING		5. TYPE OF REPORT & PERIOD COVERED 6. PERFORMING ORG. REPORT NUMBER RPI CS 79-5 ✓
7. AUTHOR(s) D. Kujawski and E. Krempl		8. CONTRACT OR GRANT NUMBER(s) N00014-76-C-0231 ✓
9. PERFORMING ORGANIZATION NAME AND ADDRESS Department of Mechanical Engineering, Aeronautical Engineering & Mechanics ✓ Rensselaer Polytechnic Institute, Troy, NY 12181		10. PROGRAM ELEMENT, PROJECT, TASK AREA & WORK UNIT NUMBERS
11. CONTROLLING OFFICE NAME AND ADDRESS Dept. of the Navy, Office of Naval Research Structural Mechanics Program Arlington, VA 22217		12. REPORT DATE December 1979 13. NUMBER OF PAGES 38
14. MONITORING AGENCY NAME & ADDRESS *(if different from Controlling Office)* Office of Naval Research - Resident Representative 715 Broadway - 5th Floor New York, NY 10003		15. SECURITY CLASS. *(of this report)* Unclassified 15a. DECLASSIFICATION/DOWNGRADING SCHEDULE

16. DISTRIBUTION STATEMENT *(of this Report)*

Approved for public release; distribution unlimited

17. DISTRIBUTION STATEMENT *(of the abstract entered in Block 20, if different from Report)*

18. SUPPLEMENTARY NOTES

19. KEY WORDS *(Continue on reverse side if necessary and identify by block number)*

Titanium alloy, room temperature, rate effects, creep, relaxation, viscoelasticity, viscoplasticity

20. ABSTRACT *(Continue on reverse side if necessary and identify by block number)*

Uniaxial tests using a servocontrolled testing machine and strain measurement at the gage length were performed on a high-strength, low-ductility, Titanium Alloy. Tests involved monotonic and cyclic loadings with strain rates between 2×10^{-8} to 10^{-3} s^{-1}, stress rates from 10^{-1} to 10^{2} MPa s^{-1} and short-term relaxation and creep tests. The inelastic behavior is strongly rate-dependent. Ratchetting is shown to increase as the stress rate decreases. No strain-rate history effect was found. A unique stress-strain curve is

DD FORM 1 JAN 73 1473 EDITION OF 1 NOV 65 IS OBSOLETE

Unclassified

SECURITY CLASSIFICATION OF THIS PAGE *(When Data Entered)*

20. Abstract (continued)

ultimately reached for a given strain rate irrespective of prior history as long as only positive stresses are imposed. In the plastic range the relaxation drop in a given time period depends only on the strain rate preceding the test and is independent of the actual stress and strain. The results are qualitatively in accordance with the viscoplasticity theory based on total strain and overstress.